J. Materials, Conc. Struct., Pavements., JSCE, No. 538/V-31, 215-225, 1996 May

SIZE EFFECT ANALYSIS FOR FLEXURE AND SHEAR STRENGTH OF CONCRETE BEAMS UNDER VARIOUS LOADING CONDITIONS BY FICTITIOUS CRACK MODEL

Ahmed Saad Eldin MORGAN[1], Junichiro NIWA[2] and Tada-aki TANABE[3]

[1]Member of JSCE, Dept. of Civil Eng., Nagoya University (Furo-cho , Chikusa-ku, Nagoya 464-01, JAPAN)
[2]Member of JSCE, Dr. of Eng., Associate Professor, Dept., of Civil Eng., Nagoya University
[3]Member of JSCE, Dr. of Eng., Professor, Dept., of Civil Eng., Nagoya University

The behavior of concrete and reinforced concrete structures is significantly affected by their sizes. The size effect on flexure and shear strengths of concrete beams has been already confirmed experimentally. This paper presents some results of the size effect on flexure and shear failures for different concrete and reinforced concrete beam sizes subjected to concentrated and uniformly distributed loads. The analysis was carried out by a computer simulation using the program ANACS (Advanced Nonlinear Analysis of Concrete Structures). Using the arc-length method the post peak behavior can be predicted well even for snap back instability.

Key Words : *concrete fracture, size effect, finite element, discrete model, fictitious crack, plain concrete, reinforced concrete, flexure strength, shear strength, rod elements.*

1. INTRODUCTION

The size effect is for design engineer probably the most compelling reason for using fracture mechanics. The size effect is defined through a comparison of geometrically similar structures of different sizes. A dependence of nominal stress at ultimate load on the structure size is called the size effect. Thus, for example the flexure failure of plain concrete beams cannot be described by the tensile strength only. More objective failure criterion for concrete appears to be the fracture energy needed for the crack propagation. These facts were recently intensively investigated and published in many proceedings[1),2)]. The introduction of fracture energy makes it possible to explain the size effect, which is observed experimentally. Due to the fact that the smeared crack model has a fundamental drawback, that is, the propagation of concrete crack is depend on the element size. Also, as pointed out by[3),4)], it is doubtful that the smeared model can be suitable to simulate a localization of fracture and unloading behaviors of concrete due to stress locking phenomenon and other reasons. Thus, in this paper discrete crack model is adopted. The tensile fracture is clearly a process of structure failure, where a discrete crack is formed in continuum and its solution is dependent on loading and boundary conditions. In fact, lumping all nonlinear deformation into interface elements involves a mechanism of softening lines or softening hinges to be assumed, similar to the assumption of yield lines or plastic hinges in the theory of plasticity. This process can be described by the fictitious crack model with two orthogonal rod elements, which implies the localization of crack[5)]. The advantage of this formulation is that it can solve a problem of discontinua with the help of the standard finite element method.

The authors have developed the fictitious crack model which was initially introduced by Hillerborg et al.[6)]. This model uses an energy based approach to predict the formation of cracks in concrete. In this approach the fracture energy of concrete, G_F is associated with a stress-crack width curve. This approach shows that the fictitious crack model combined with arc-length method is capable of describing the size effect even in post peak brittle

failure in flexure and shear problems in concrete and reinforced concrete beams, respectively. Because of using arc-length method which depends on load control approach, the problems where the structure is subjected to more than one external loads at different node points such as case of uniformly distributed loads can be analyzed by the current program (ANACS).

In the standard specification for design and construction of concrete structures of JSCE the design equation considering the size effect was already specified. The present paper documents these experiences on calculations made in connection with JSCE provisions of the size effect analysis in concrete structures. The comparison with experiments is not presented. However, such a comparison can be certainly done for the small size beams, but for the huge size beams it is virtually impossible to perform the experiments.

2. FINITE ELEMENT MODELING FOR CONCRETE AND STEEL ELEMENTS

The complete and detailed discussion of the ANACS program is exceeding the range of this paper, and therefore only main principles are mentioned here and a detailed description is devoted only to the fracture modeling, which is prevailing in the analyzed cases. The ANACS program has a complete finite element armory which has 4,5,6,7, and 8 noded quadrilateral elements. Also, 3, and 6 noded triangular elements have been incorporated into the program in order to provide for mesh grading and flexibility in mesh construction.

Concrete elements are elastic in tension. Therefore, the flexure and shear cracks can be easily localized based on the fictitious crack approach by using the two orthogonal rod elements. Concrete elements in compression is modeled by bilinear stress strain curve as shown in **Fig.1**.

The adopted criterion for detecting crushing of concrete elements is governed by the biaxial compression yield surface proposed by Kupfer et al.[7]; **(Fig.2)**.

A two noded truss element for reinforcement simulation is proposed with a bilinear stress strain relation **(Fig.3)**. Each node of this element has two degrees of freedom. This element is connected directly to the concrete element.

Due to the fact that the studied cases in this paper concern with flexure failure and diagonal tension failure of concrete and reinforced concrete

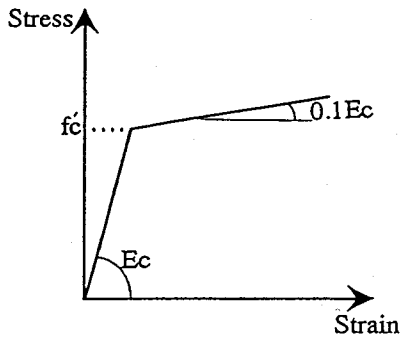

Fig.1 Concrete model in compression

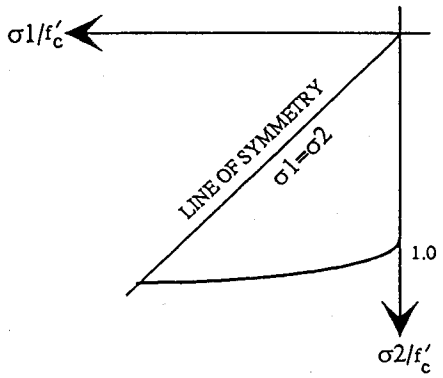

Fig.2 Biaxial compressive strength envelope for concrete

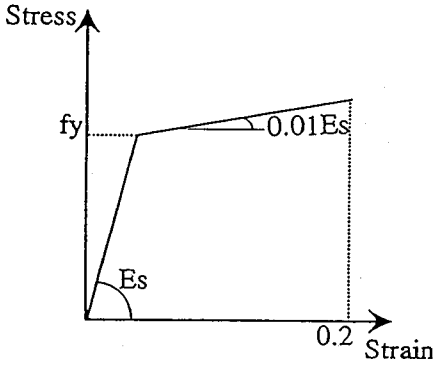

Fig.3 Steel model

beams, respectively, thus compressive stresses in concrete and the tensile stresses in steel are always within the elastic range.

The program ANACS is developed to reduce the bulky input material by incorporating two dimensional generation for the finite element mesh

for all types of quadrilateral and triangular elements, steel bars, and nodal coordinates. Also, the program involves an interface graphical post processor to generate the mesh geometry, and deformed shapes through Autocad package. These facilities are useful for detecting the mesh geometry, and the failure modes.

3. FICTITIOUS CRACK SIMULATION FOR CONCRETE

The fracture zone was modeled by two orthogonal rods between the pairs of decoupled nodes of concrete elements along a priori chosen crack path. **Fig.4** shows the two orthogonal rods which are used to simulate the crack and represent the localized crack zone. In the present model, one of the rod elements was taken parallel to the X-axis, and the other one was taken parallel to Y-axis disregarding the crack path orientation. In other words, the linkage elements will have a certain orientation does not matter how the crack path inclination is, as shown in **Fig.4**. Moreover. this formulation of these linkage elements will not disturb the fracture energy balance, which is independent on the fictitious crack orientation. For more justification refer to Appendix A. The horizontal rod element exhibits non linear stress-strain behavior of concrete by using the 1/4th softening curve. For this rod element, the tensile fracture energy remains constant and is equal to 100N/m as a representative value of the fracture energy which is used in many researches[8]. The length of rod element is assumed as unity (L=1).

Using the 1/4th model curve **(Fig.5)** for horizontal rod element, the strain can be calculated which is equivalent to the crack width and then the corresponding stress can be obtained. Also, the compression bilinear curve is incorporated to the previous model to simulate the rod element under compression as shown in **Fig.5**.

The stiffness matrix of this horizontal rod element is given using the force displacement relation in the global system of axes as follows:

$$\begin{bmatrix} F_x^i \\ F_y^i \\ F_x^j \\ F_y^j \end{bmatrix} = \frac{A_C E_C}{L} \begin{bmatrix} 1 & 0 & -1 & 0 \\ 0 & 0 & 0 & 0 \\ -1 & 0 & 1 & 0 \\ 0 & 0 & 0 & 0 \end{bmatrix} \begin{bmatrix} u^i \\ v^i \\ u^j \\ v^j \end{bmatrix} \qquad (1)$$

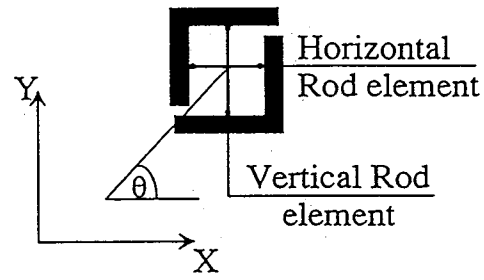

Fig.4 The rod elements for crack simulation

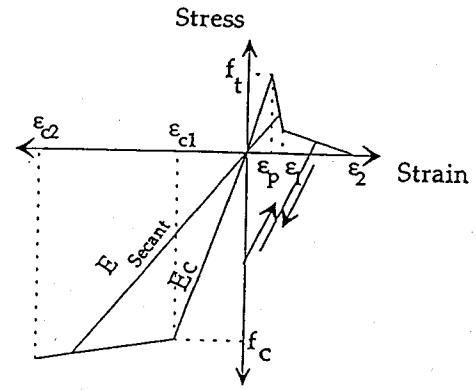

Fig.5 Stress-strain model for horizontal rod element

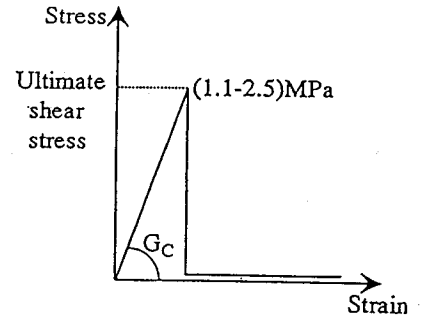

Fig.6 Stress-strain model for vertical rod element

where A_c is the area of concrete served by this rod element, L is the length of rod element and E_c is the Young's modulus of concrete.

Since the vertical rod element which represents the shear sliding is perpendicular to the previous one, the stiffness matrix for this rod element can be considered as follows:

$$\begin{bmatrix} F_x^i \\ F_y^i \\ F_x^j \\ F_y^j \end{bmatrix} = \frac{A_C G_C}{L} \begin{bmatrix} 0 & 0 & 0 & 0 \\ 0 & 1 & 0 & -1 \\ 0 & 0 & 0 & 0 \\ 0 & -1 & 0 & 1 \end{bmatrix} \begin{bmatrix} u^i \\ v^i \\ u^j \\ v^j \end{bmatrix} \quad (2)$$

where A_C and L are the same as before, and G_C is the shear modulus of concrete.

For the 1/4th tension model,

$$\varepsilon_p = \frac{f_t}{E_C} \qquad \varepsilon_1 = 0.75\frac{G_F}{f_t} \qquad \varepsilon_2 = 5\frac{G_F}{f_t} \quad (3)$$

$$\sigma = \begin{cases} E_C\varepsilon & 0 < \varepsilon \le \varepsilon_p \\ f_t - \dfrac{0.75 f_t(\varepsilon - \varepsilon_p)}{\varepsilon_1 - \varepsilon_p} & \varepsilon_p < \varepsilon \le \varepsilon_1 \\ \dfrac{f_t}{4} - \dfrac{f_t(\varepsilon - \varepsilon_1)}{4(\varepsilon_2 - \varepsilon_1)} & \varepsilon_1 < \varepsilon \le \varepsilon_2 \\ 0 & \varepsilon_2 < \varepsilon \end{cases} \quad (4)$$

$$E_R = \begin{cases} E_C & 0 < \varepsilon \le \varepsilon_p \\ E_{Secant} & \varepsilon_p < \varepsilon \le \varepsilon_2 \\ 0.00001E_C & \varepsilon_2 < \varepsilon \end{cases} \quad (5)$$

For the compression model,

$$\sigma_{comp.} = -\begin{cases} E_C|\varepsilon_{c1}| & 0 < |\varepsilon| \le |\varepsilon_{c1}| \\ f_c' + 0.1E_C\left(\dfrac{|\varepsilon| - |\varepsilon_{c1}|}{|\varepsilon_{c2}| - |\varepsilon_{c1}|}\right) & |\varepsilon_{c1}| < |\varepsilon| \le |\varepsilon_{c2}| \\ 0 & |\varepsilon_{c2}| < |\varepsilon| \end{cases} \quad (6)$$

$$E_{comp.} = \begin{cases} E_C & 0 < |\varepsilon| \le |\varepsilon_{c1}| \\ E_{Secant} & |\varepsilon_{c1}| < |\varepsilon| \le |\varepsilon_{c2}| \\ 0.00001E_C & |\varepsilon_{c2}| < |\varepsilon| \end{cases} \quad (7)$$

where f_t and f'_c are the tensile, and compressive strength of concrete, respectively, G_F is the fracture energy of concrete, and E_R is the elasticity modulus of the rod element in tension model which takes different values according to different strain stages as defined by Eq.(5), Similarly, the E_{comp} is the elasticity modulus of the rod element in compression model and its value are defined by Eq.(7).

Also, to have a realistic model, unloading and reloading phenomenon was incorporated into the tension model for the horizontal rod element.

The stress-strain relation for vertical rod element is taken as linear elastic till the tensile stress in the horizontal rod element exceeds the tensile strength of concrete. Thus, when the crack starts at a certain horizontal rod element, the resistance of the corresponding vertical rod element vanishes.

Due to the fact that the fracture energy model to define the shear stresses by the vertical rod element is not known, thus a very simple model as shown in **Fig.6** was chosen. Moreover, according to the adopted formulation for those orthogonal rod elements the ultimate shear stress for the vertical rod element can be taken as any value ranges between (1.1~2.5)MPa. This wide range of chosen ultimate shear stress for vertical rod model **(Fig.6)** reflects that the crack formation and propagation, and the ultimate shear strength of the studied reinforced concrete beams mainly depend on the tensile fracture energy stored in the horizontal rod element which is defined by 1/4th softening model **(Fig.5)**.

At advanced stages of fracture zone development, the compressive stress in the upper part of the beam becomes large, in both rod elements. Then, when the absolute value of the shear stress in the vertical rod element exceeds the predefined ultimate shear stress **(Fig.6)**, the stresses in both orthogonal rod elements are vanished, i.e. the both rod elements lose all their stiffness.

4. NUMERICAL SOLUTION TECHNIQUE FOR NONLINEAR ANALYSIS

The current analysis is tried to trace the entire load-deformation response of the concrete structures. However, tracing of limit point and post limit path is notoriously difficult especially for structures which have a response involving a snap back behavior. However, it is important to know whether the structure collapse is a ductile or a brittle form, and to define a material modeling including the softening behavior. Then, the establishment of arc-length procedure[9] is necessary for dealing with overcoming limit points in a nonlinear solution path.

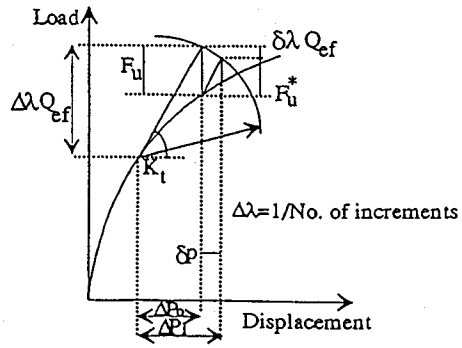

Fig.7 The spherical arc-length procedure

Moreover, a technique has been adopted[10] to maintain the symmetric banded nature of the equilibrium equations.

The basic idea in all arc-length methods is to modify the load level at each iteration, rather than holding the applied load level constant during a load step, so that the solution follows some specified path until convergence is attained.

The procedure of the arc-length method will be reviewed briefly as follows.

As shown in **Fig.7** the out of balance force vector at the beginning of any iteration is

$$F_u^* = F_u - \delta\lambda Q_{ef} \tag{8}$$

where F_u^* is the unbalanced force of this iteration, and F_u is the unbalanced force of last iteration.

Then the iterative displacement δP is

$$\delta P = K_t^{-1} F_u^* = -\delta\lambda K_t^{-1} Q_{ef} + K_t^{-1} F_u = \delta\lambda \delta P_t + \delta\overline{P} \tag{9}$$

where $\delta\overline{P}$ is the standard iterative change for some known unbalanced forces, and K_t is the tangent stiffness matrix at beginning of the load increment, while δP_t is the displacement vector, and Q_{ef} is the total external load vector.

The new incremental displacement vector is

$$\Delta P_1 = \Delta P_o + \delta P = \Delta P_o + \delta\overline{P} + \delta\lambda \delta P_t \tag{10}$$

In Eq.(10) δλ is the only unknown. The main essence of the arc-length methods is that the load parameter δλ becomes a variable. Hence, together with n displacement variables, we have a total of n+1 variables. For these variables, we have n equilibrium equations and the one constraint equation by fixing the incremental length ΔL in n dimensional space, i.e.

$$\Delta L^2 = \Delta P_1^T \Delta P_1 \tag{11}$$

Substitute Eq.(10) into Eq.(11) gives the following scalar quadratic equation

$$a_1 \delta\lambda^2 + a_2 \delta\lambda + a_3 = 0 \tag{12}$$

Where

$$a_1 = \delta P_t^T \delta P_t \tag{13}$$

$$a_2 = 2\delta P_t (\Delta P_o + \delta\overline{P}) \tag{14}$$

$$a_3 = (\Delta P_o + \delta\overline{P})^T (\Delta P_o + \delta\overline{P}) - \Delta L^2 \tag{15}$$

To solve for Eq.(12), the value under the square root of Eq.(16) should be greater than zero.

$$\delta\lambda = \frac{-a_2 \pm \sqrt{a_2^2 - 4a_1 a_3}}{2a_1} \tag{16}$$

The choice of root in Eq.(16) can be referred to[11].

As a result of some troubles, which can be generated from many sources such as the reversible displacements (see chapter 5), the value of a_3, which depends on $\delta\overline{P}$, will be highly increased. Then, the value under the root will be negative, consequently the program will fail to carry out any further calculations.

5. TENSILE FAILURE OF PLAIN CONCRETE BEAMS IN BENDING

The concrete beam geometry is illustrated in **Fig.8**. Six different sizes are considered h=0.1, 0.5,1.0,2.0,3.0, and 5.0m. The concrete properties are identical for all six beams: f'_c=30.0MPa, f_t=3.0MPa, G_F=100N/m, and E_c=30.0GPa.

Only symmetrical half of the beam was analyzed in order to avoid the reversible displacement after the crack begins to open which leads to numerical instability and lack of convergence through

arc-length calculation procedure. If the two halves of the beam are considered in the analysis, the reversible displacements will be generated when the other half of the beam moves after cracking in the opposite direction to its movement before cracking.

Also, the rod elements are incorporated through the flexural crack. Actually, there is no shear stress along this flexure crack, but the incorporation of the rod element which parallels to crack path is needed to maintain the structure stability against any vertical forces produced by numerical calculations such as unbalanced forces. Also, as shown in **Fig.8** both 4, and 5 nodded elements are used to facilitate mesh grading near the beam center line. Further, it is noticed that the numerical instabilities through the calculations are reduced as much as the rod elements is used along the crack path, because the stiffness matrix has a gradual change, therefore, no sudden change in the over all structure stability configuration occurs, which leads to numerical instability, and lack of convergence. Thus, the mesh was graded fine near the center line predefined crack, with 20 elements over the beam depth, and then 41 rod elements are used along the crack path with the help of 5 nodded transition element. Two sets of calculations are performed. One is concentrated load at distance 2h from the support as shown in **Fig.8**, and the other is uniformly distributed loads along the top surface of the beam.

The failure was initiated by formation of a fracture process zone with a discrete crack in the region of tensile stresses. The solution was done by the arc-length control, and the post peak behavior can be achieved as shown in **Fig.9** which shows the load-displacement diagram of beam size 50cm with a post peak snap back response in both cases of loading. While **Fig.9** presents the shear force versus displacement diagram for the total shear force at the support, and the displacement at loading point in case of concentrated load, the same relation is described for the case of uniformly distributed load. Moreover, In case of uniformly distributed load, much smaller intervals near the peak load were tried, but the structure cannot sustain any small interval beyond the existed peak, and the load-displacement response starts to turn down.

Fig.10 shows the tendency of ultimate strength to decrease with the increase of beam size in both cases of loading. This behavior is known as the size effect. Also, as shown in **Fig.10** the size effect is moderated for large heights, and the peak stress of the beams tends to become equal to tensile strength of concrete. By comparing the results of both sets it

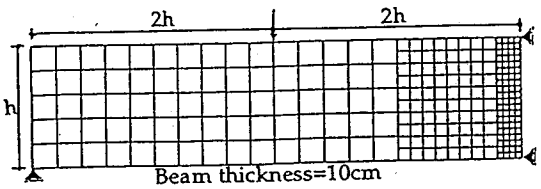

Fig.8 The mesh for plain concrete beams

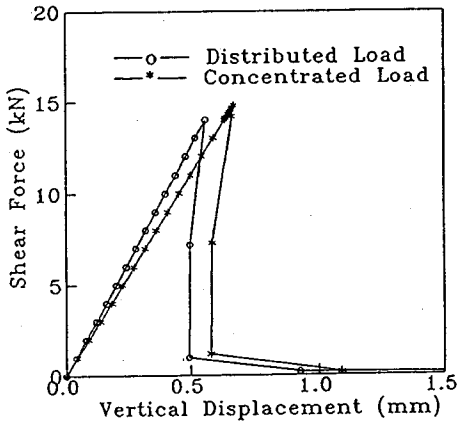

Fig.9 Shear force versus displacement diagram for both loading cases

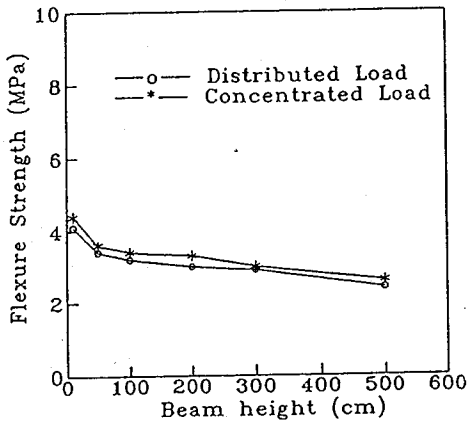

Fig.10 Size effect in flexural strength

was found that in case of the concentrated load at distance 2h from the support, the ultimate strength due to applying uniformly distributed loads is smaller than that in the case of applying concentrated load by about 5%.

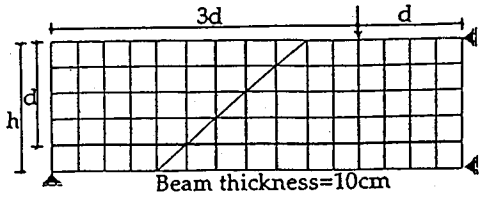

Fig.11 The mesh for reinforced concrete beams

6. SHEAR FAILURE OF REINFORCED CONCRETE BEAMS WITHOUT STIRRUPS

The adopted mesh and the geometry of the studied reinforced concrete beams are shown in **Fig.11**. Both 6 noded triangular elements, and 8 noded quadrilateral elements are utilized. Six beam sizes are considered from 0.1 to 5.0 m.

Also, two sets of calculations are performed. One is concentrated load and the other is uniformly distributed load. They are only reinforced with the longitudinal bars at depth d equal to 0.8 the beam height, i.e. there is no vertical stirrups. The beams are geometrically similar. For all beams the reinforcement ratio is 2%, and the ratio of shear span to beam depth was set to 3.0 in case of concentrated load. The concrete properties identical for all six beams are: f'_c=30.0MPa, f_t=3.0MPa, G_F=100N/m, and E_c=30.0GPa. The reinforcement has the yield strength f_y=400.0MPa, and Young's modulus E_s=210.0GPa. For performing more realistic analysis, the beams are analyzed with multicrack that is diagonal shear crack together with flexure crack along the beam centerline **(Fig.12)**.

Based on extensive parametric study the inclination of the diagonal shear crack was determined. The diagonal shear crack was oriented at angles 32°,35°,40°, and 45°, then a new finite element mesh was rearranged with respect to the chosen path. However, it was found that the inclination of 40° gives the minimum shear strength **(Fig.13)**, so this angle was selected for further calculations. The location of the fictitious crack which gives the minimum shear strength was found at distance (d) from the support[5]. Therefore, in this paper the shear crack was chosen at distance (d) from the support. Also, it is better to mention that in case of uniformly distributed load the detected shear strengths in **Figs.13,14**, and **15** are calculated based on the shear force at the support position.

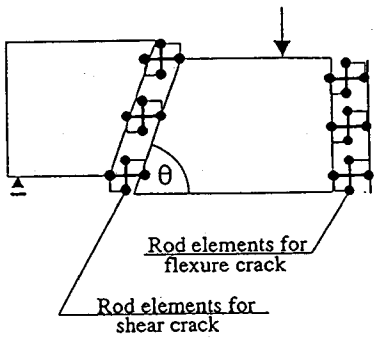

Fig.12 Schematic diagram to illustrate the proposed crack planes

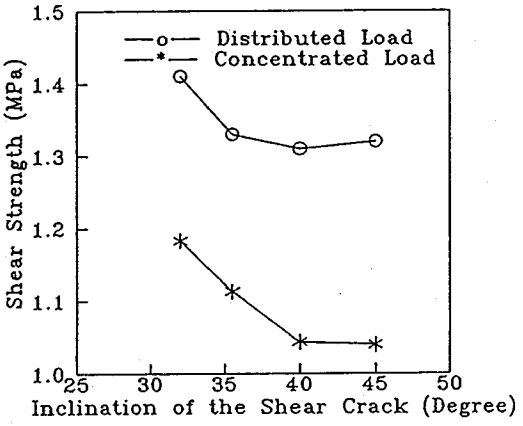

Fig.13 Variation of ultimate shear strength with shear crack inclination

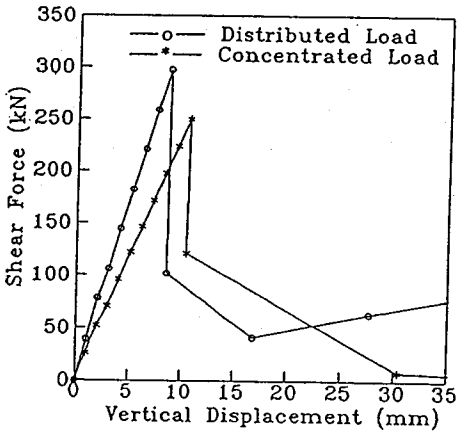

Fig.14 Shear force versus displacement diagram for both loading cases

The analysis was done by the arc-length control and was stable in all cases in the whole softening range as shown in **Fig.14** which shows the shear force versus displacement diagram of beam size 3.0m with a post peak snap back response. By the way in **Fig.14** the detected point for examining the vertical displacement is the loading point in case of concentrated load, for the sake of comparison the same point is considered in case of uniformly distributed load. Also, in **Fig.14** much smaller intervals were tried, but they also showed the same peak values.

The fracture softening properties of **Fig.14** shows that for large sizes such as h=3.0m, failure becomes brittle and the snap back behavior occurs. The snap back phenomenon occurs because there is a sudden bifurcation process which leads to a sudden drop in both load and deflection. In other words, fracture of concrete leads to brittle failures and as a result causes the size effect of decreasing strength in structures of increased sizes.

Also, the results of this study with design equation of **JSCE** are illustrated in **Fig.15**. According to this figure, the tendency of shear strength to decrease with the increase in the beam size has been obtained. Moreover, **Fig.15** shows that our calculations in case of concentrated load has almost a full agreement with **JSCE** design equations for beams within 1.0m height. However, as shown in **Fig.15** the size effect disappears at large depths. In such beams, the softening tensile stress has a major significance because the deformation in the failing crack is governed by crack opening as shown later in **Fig.18.**

Shear stresses across the fracture zone carried by aggregate interlocking between fracture surfaces were not considered, nor was the shear force carried by dowel action of the reinforced steel considered. These assumptions mean that the calculated shear strength becomes conservative. Concerning the aggregate interlocking, it is mentioned that for slender reinforced concrete beams without shear reinforcement under shear load, the aggregate interlock has a minor significance in the shear resistance due to post cracking shear mechanism[12].

By comparing the peak stresses of both cases of loading it is found that the calculated shearing force and bending moment at the location where the diagonal tension crack generates at the lower edge of the beam, i.e. at distance (d) from the support[5], are almost the same for both loading cases, and it does not mater how the load configuration is. This means that the crack will begins to open when the

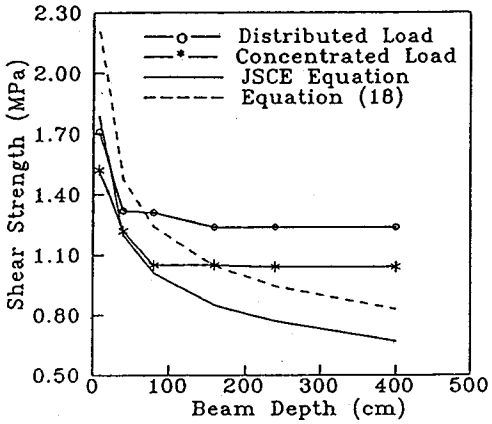

Fig.15 Comparison of shear strength analysis with ANACS program for both cases of loading, JSCE equation, and the proposed equation

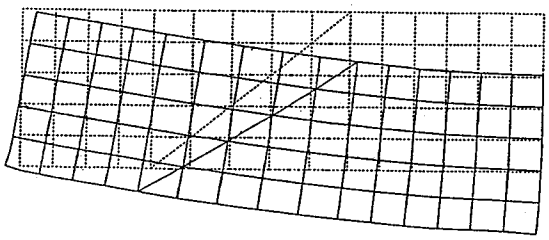

Fig.16 Deformed shape at the peak load

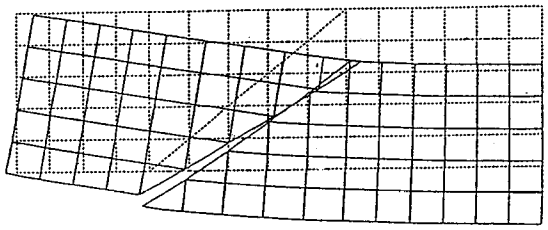

Fig.17 Deformed shape for the first increment after the peak load

stresses at crack location reach to a certain limit disregarding the loading condition. Referring to the **JSCE** equation which is used to predict the ultimate shear strength of simply supported beam with concentrated load[13], the authors hit on the idea to extent this equation to apply it in case of uniformly distributed load.

The JSCE equation for concentrated load is as follows

$$v_C = 0.20(\rho_w f'_C)^{1/3} d^{-1/4}[0.75+1.4/(a/d)] \quad (17)$$

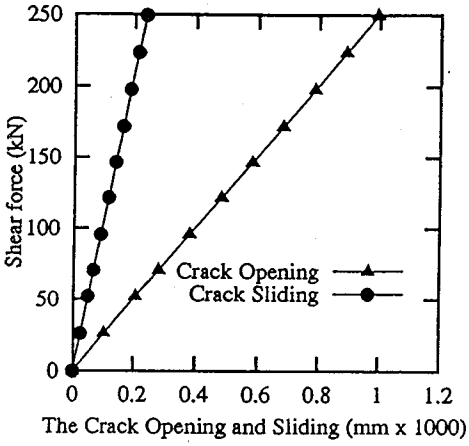

Fig.18 The shear force versus both the crack opening and the crack sliding case of concentrated load

where v_c is the ultimate shear strength (MPa), f'_C is the compression strength (MPa), $\rho_w = 100A_S/(b_w d)$, b_w is the breadth of web, A_S is the cross sectional area of tensile reinforcing bars, a is the shear span, and d is the effective depth (m).

Then, if we choose a/d≅3.0[13] and substitute in Eq.(17), we can write the ultimate shear strength equation as follows

$$v_C = 0.3(\rho_w f'_C)^{1/3} d^{-1/4} \qquad (18)$$

Finally, in case of uniformly distributed load and the span to depth ratio (l/d) about 8.0, the ultimate shear strength can be roughly estimated from Eq.(18), which takes into account the size effect in the term of $d^{-1/4}$.

Furthermore, **Fig.16** and **Fig.17** show the deformed shapes at the peak load and at the next increment after the peak of the beam 3.0m height in case of concentrated load. It can be noticed that the displacements at beam axis of symmetry and around loading point in **Fig.17** is smaller than that of **Fig.16**, which illustrates the effect of snap back phenomenon. For **Figs.16,17** the deformed shapes are drawn with magnification factor equals to 100.

From **Fig.18** it was found that in the diagonal shear crack failure, the crack opening was much larger than the crack sliding, which reflects that the shear failure is a matter of mode I fracture of concrete and the size effect is caused primarily by concrete fracture. **Fig.18** shows the crack opening and the crack sliding response at distance (d) from the support up to the failure load of beam height 3.0m.

7. CONCLUSIONS

It is possible to study the influence of different variables on flexure, and shear strength theoretically by means of nonlinear fracture mechanics for different loading cases. In particular, fracture mechanics offers a possibility to explain the size effect in both flexure and shear strengths. It was observed that for smaller beams till 100cm height the shear capacity of beams having only flexure reinforcement is profoundly affected by size effect in both concentrated and uniformly distributed loading. On the other hand, beams with height more than 100cm the numerical predictions showed that the size effect becomes negligible. Moreover, the snap back phenomenon occurs when the beam size increases and the brittle behavior of concrete beams becomes significant. The failure due to diagonal cracking is a matter of mode I fracture energy. In the case of diagonal tension failure, the bending moment values which is calculated at the peak load in both loading cases at the crack location are almost the same, disregarding how the load configuration is. This means that the crack will begin to open when the stresses at crack location reach to a certain limit irrespective of the history of the loading condition. Also, it is found that the inclination of 40^0 gives the minimum shear strength in both loading cases. The ultimate flexure strength due to applying uniformly distributed load is smaller than the case of applying concentrated load by about 5%. Finally, the results of JSCE equation for shear strength is more or less conservative for extremely large beams.

APPENDIX A ROD ELEMENTS ORIENTATION

The reasons for using such fixed orientation of the rod elements are as follows:

A) In case of simulating both flexure and shear cracks, the crack was implemented from early beginning along over the whole beam depth. Moreover, naturally a compression zone at the top of the beam will be created. Then if the rod elements are incorporated as one parallel to crack and the other one perpendicular to crack, it was found that the compression strains in the compression zone will create displacements along both rod elements producing high forces in the rod element which is parallel to the crack. On the other hand the fracture energy model to define shear stress

by mode II of failure was not available to control or define such high forces generated in this parallel to crack rod element (**Fig.A-1**). Furthermore, if any kind of models for this rod elements was proposed, it was found that the resulting peak load was highly dependent on the chosen model[14]. Finally, it was found that , the using of the proposed expression of the rod elements can overcome such problems, because in the compression zone, these compression strains will not generate any significant forces in the vertical rod element.

For more explanation, the free body diagram in **Fig.A-1** shows that in case of using perpendicular, and parallel rod elements concept, even after yielding all rod elements in the tension zone, there is a reasonable force generated in the parallel to crack rod element F_P, which it can stabilize the free body as much as the load is applied on the beam.

B) In another case where parallel, and perpendicular rod elements concept is applied to the direct tension test **Fig.A-2**. It can be found that if a simple tension force was applied, at one end, then the beam will have sliding along the crack path, in stead of direct crack opening.

Fig.A-3 shows two orthogonal rod elements inclined with angle θ, and the stiffness of the rod elements was taken as Young's modulus E and the shear modulus G for the perpendicular and the parallel to crack rod elements, respectively. Only one horizontal tension force was considered.

From **Fig.A-3** the following equilibrium equations can be obtained.

$$\frac{A_C}{L}\begin{bmatrix} C^2+ES^2 & GSC-ECS & -C^2-ES^2 & -GCS+ECS \\ GSC-ECS & S^2+EC^2 & -GCS+ECS & -S^2-EC^2 \\ -C^2-ES^2 & -GSC+ECS & C^2+ES^2 & GSC-ESC \\ -GCS+ECS & -S^2-EC^2 & GSC-ECS & S^2+EC^2 \end{bmatrix}\begin{bmatrix} U_1 \\ V_1 \\ 0 \\ 0 \end{bmatrix}=\begin{bmatrix} P \\ 0 \\ F_{U2} \\ F_{V2} \end{bmatrix} \quad \text{(A-1)}$$

where E and G are the Young's modulus, and the shear modulus of concrete, Respectively, S = sinθ, and C = cosθ.

By subdividing these equilibrium equations, then

$$\frac{L}{A_C GE}\begin{bmatrix} GS^2+EC^2 & ECS-GSC \\ ECS-GSC & GC^2+ES^2 \end{bmatrix}\begin{bmatrix} P \\ 0 \end{bmatrix}=\begin{bmatrix} U_1 \\ V_1 \end{bmatrix} \quad \text{(A-2)}$$

$$\therefore \frac{L}{A_C GE}\left(GS^2+EC^2\right)P=U_1 \quad \text{(A-3)}$$

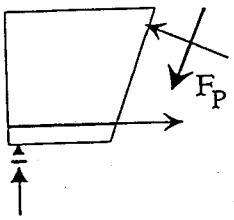

Fig.A-1 Schematic diagram to illustrate the effect of F_P

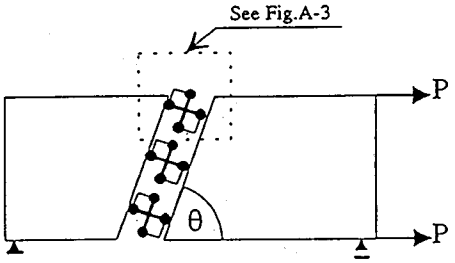

Fig.A-2 Schematic diagram shows simple tension test with rod elements

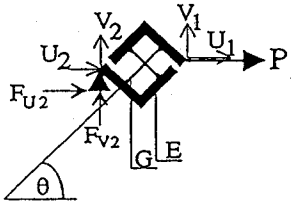

Fig.A-3 Structural simulation for the linkage elements

$$\therefore P=\frac{A_C GEU_1}{L}\frac{1}{\left(GS^2+EC^2\right)} \quad \text{(A-4)}$$

If θ is equal to 90° i.e. G's rod element will be vertical (parallel to Y-axis), E's rod element will be horizontal (parallel to X-axis), the Eq.(A-4) will be;

$$\therefore P=\frac{A_C EU_1}{L} \quad \text{(A-5)}$$

From Eq.(A-4) it was found that the force P which required to make a unit displacement will highly depends on the inclination angle θ, and E/G ratio. Thus if θ=90° is substituted in Eq.(A-4), then the force P will be tackled only by the tensile flexure rod element as shown by Eq.(A-5).

Also, the following equation can be written for V_1

$$\therefore V_1 = \frac{L}{A_C GE}(ECS - GCS)P \qquad \text{(A-6)}$$

By substituting θ=90° in Eq.(A-6), it was found that $V_1 = 0$, which can be considered the most realistic behavior of these rod elements, because the structure is subjected to only horizontal force P. If this horizontal force produces vertical displacement then the behavior of these rod elements will reflect unrealistic behavior of the analyzed beams.

REFERENCES

1) Bazant, Z.P., editor: Fracture Mechanics of Concrete Structure, *Proceedings of the First International Conference FraMCos1*, Colorado, USA, 1-5 June, 1992.
2) van Mier, J.G.M., editor: Fracture Processes in Concrete, Rock and Ceramics, *Proceedings of the International RILEM/ESIS Conference*, Noordwijk, Netherlands, June 19-21, 1991.
3) Shirai, N.: JCI Round Robin Analysis in Size Effect in Concrete Structures, *JCI International Workshop on Size Effect in Concrete Structures*, Sendai, Japan, pp. 247-270, Oct., 1993.
4) Rots, J.G. and Blaauwendraad, J.: Crack Models for Concrete: Discrete or Smeared? Fixed, Multidirectional or Rotating?, *Heron*, Vol.34, No.1, p. 59, 1989.
5) Niwa, J., et al.: Size Effect Analysis for Shear Strength of Concrete Beams Based on Fracture Mechanics, *J. of M.C.S.P. of JSCE*, No.508/V-26, pp. 45-53, Feb., 1995.
6) Hillerborg, A., Modeer, M. and Peterson, P.E.: Analysis of Crack Formation and Crack Groth in Concrete by Means of Fracture Mechanics and Finite Element, *Cement and Concrete Research*, pp. 773-782, Vol. 6, 1976.
7) Kupfer, H. and Crestle, K.H.: Behavior of Concrete under Biaxial Stresses, *ASCE*, Vol.99, No. EM4, pp. 853-866, Aug., 1973.
8) RILEM TC 90-FMA : Fracture Mechanics of Concrete - Applications, *Round Robin Analysis of Anchor Bolts, Preliminary Report*, 2nd ed., May, 1991.
9) Riks, E.: An Incremental Approach to the Solution of Snapping and Buckling Problems, *Int. J. Solids Struct.*, 15, pp. 524-551, 1979.
10) Batoz, J.L. and Dhatt, G.: Incremental Displacement Algorithms for Nonlinear Problems, *Int. J. Num. Meth. Engng*, 14, pp. 1262-1266, 1979.
11) Crisfield, M.A.: Non-linear Finite Element Analysis of Solid and Structure, *John Wiley & Sons*, Vol.1, 1991.
12) Wang, Q.B. and Blaauwendraad, J.: Consequence of Concrete Fracture: Brittle Failure and Size Effect of R.C. Beams Under Shear, *Proceedings of the International RILEM/ESIS Conference*, Noordwijk, Netherlands, June 19-21, 1991.
13) Niwa, J., et al.: Revaluation of the Equation for Shear Strength of Reinforced Concrete Beams without Web Reinforcement, *Concrete library of JSCE*, No. 9., pp. 65-84, June, 1987.
14) Morgan, A.S.E. and Niwa, J.: Analysis of Size Effect in Concrete Structures, *Proc. JCI*, Vol. 17, No.2, pp. 1335-1340, 1995.
15) Morgan, A.S.E., Niwa, J. and Tanabe, T.: Size Effect Analysis for Shear Strength of Beams by Fractures Mechanics, *Proc. EASEC-5*, Griffith University, Gold Coast, Australia, Vol.1, pp. 621-626, 1995.

(Received May 8, 1995)

仮想ひび割れモデルを用いた各種荷重条件下のコンクリートはりの曲げおよびせん断強度の寸法効果

Ahmed Saad Eldin MORGAN・二羽淳一郎・田邊忠顕

コンクリートおよび鉄筋コンクリート構造物の挙動は，その寸法に強く影響される．コンクリートはりの曲げおよびせん断強度の寸法効果は既に実験的に確認されており，示方書にも寸法効果を考慮した設計式が規定されている．本研究は，集中荷重ならびに分布荷重を受けるコンクリートおよび鉄筋コンクリートはりの曲げおよびせん断強度の寸法効果を仮想ひび割れモデルと直交ロッド要素を用いた解析により，統一的に，破壊力学的に評価したものである．なお，ポストピーク後のスナップバック現象に対処するために，弧長法による定式化を導入している．